Environmental Science and Pollution Research (2021) 28:41191–41206
https://doi.org/10.1007/s11356-021-13695-y

RESEARCH ARTICLE

Detecting urban landscape factors controlling seasonal land surface temperature: from the perspective of urban function zones

Tong Li[1] · Ying Xu[2] · Lei Yao[1]

Received: 28 January 2021 / Accepted: 24 March 2021 / Published online: 29 March 2021

Abstract

Understanding the impact on the thermal effect by urbanization is of great significance for urban thermal regulation and is essential for determining the relationship between the urban heat island (UHI) effect and the complexities of urban function and landscape structure. For this purpose, we conducted case research in the metropolitan region of Beijing, China, and nearly 5000 urban blocks assigned different urban function zones (UFZs) were identified as the basic spatial analysis units. The seasonal land surface temperature (LST) retrieved from remote sensing data was used to represent the UHI characteristics of the study area, and the surface biophysical parameters, building forms, and filtered landscape pattern metrics were selected as the urban landscape factors. Then, the effects of urban function and landscape structure on the UHI effect were examined based on the optimal results of the ordinary least squares and geographically weighted regression models. The results indicated that (1) Significant spatio-temporal heterogeneity of the LST was found in the study area, and there was an obvious temperature gradient with "working–living–resting" UFZs. (2) All types of urban landscape factors showed a significant contribution to the seasonal LST, in the order of surface biophysical factors > building forms > landscape factors; however, their contributions varied in different seasons. (3) The major contributing factors showed a certain difference due to the variation of urban function and landscape complexity. This study expands the understanding on the complex relationship among urban landscape, function, and thermal environment, which could benefit urban landscape planning for UHI alleviation.

Keywords Urban function zones · Urban heat island · Urban landscape · Land surface temperature · Spatiotemporal heterogeneity

Introduction

Rapid urbanization has profoundly altered the underlying landscape features in urban regions, manifested as a massive transformation of natural landscapes into artificial surfaces (Grimm et al. 2008; Wang et al. 2012). This change has resulted in significantly intensive thermal absorption and release processes with ever-expanding urban built-up regions and increasing anthropogenic activities than ever before, thus leading to a severe urban heat island (UHI) phenomenon (Gago et al. 2013). As one of the most concerning urban environment issues, the growing UHI effect will induce several adverse impacts on urban and residential health, such as thermal discomfort, energy waste, air pollution, and increasing morbidity/mortality (Arnfield 2003; Ulpiani 2021; Wu and Ren 2018). Because of this, more in-depth information on the UHI effect within an urban region has drawn greater attention from urban planners and the related research community.

To better understand and solve the problem of the UHI effect, it is essential to establish its relationship with urban landscape features. To this end, both UHI and urban landscapes should be indexed reasonably for quantitative analysis. With the rapid development of thermal infrared remote sensing technology, imagery-retrieved land surface temperature (LST) has been widely recommended for representing the

Responsible Editor: Philippe Garrigues

✉ Lei Yao
alex_yaolei@126.com; yaolei@sdnu.edu.cn

Tong Li
litong19950802@126.com

Ying Xu
xuy_1986@126.com

[1] College of Geography and Environment, Shandong Normal University, Jinan 250358, China

[2] School of Civil Engineering, Shandong Jiaotong University, Jinan 250023, China

near-surface UHI in urbanized regions, in view of its merits in accurately mapping the spatial features of urban thermal environments at various spatial scales (Weng 2009). A considerable number of studies have been conducted to depict the urban landscape characteristics for assessing their relationship with the LST, enabling the classification of urban landscapes pattern as composition and configuration factors, which both have been argued to cause a significant influence on the variation of LST (Buyantuyev and Wu 2010; Chen et al. 2014a; Li et al. 2012). Landscape metrics, referring to the theory of landscape ecology, are often used to quantify the spatiotemporal changes in landscape composition and configuration when describing urban thermal complexities (Chen et al. 2012). However, traditional landscape metrics are not always optimal for analyzing landscape patterns due to metric redundancy (Chen et al. 2016) and a lack of clear ecological analogues (Kedron et al. 2018). Additional indices have thus been introduced into UHI-related studies. For example, the normalized difference vegetation index (NDVI), as one of the remote sensing-based surface biophysical parameters to characterize the status of urban green spaces, has been widely reported to have a significantly correlation with the LST (Deilami et al. 2018; Peng et al. 2018). Recently, increasing attention has been focused on the landscape factors assigned urban 2D or 3D morphology to expound the connection between urbanization and UHI with a new dimension (Yang et al. 2013).

Although the above issues have fostered discussions in the UHI field, there are still questions that require further discussion. Most of the previous studies concerning the impacts of urbanization on its thermal effect preferred regular grids or concentric buffers as the analysis units, with better accessibility and comparability for analysis (Chen et al. 2014a; Hou and Estoque 2020). However, relevant scholars believe that the use of these analysis units is often faced with the problem of choosing an appropriate spatial scale, and different types/scales of spatial analysis units may alter the thermal contributions of different types of landscape features (Zhou et al. 2014). Furthermore, the spatial expression of both urban thermal and landscape characteristics at the local scale is usually characterized by significant heterogeneity (Li et al. 2017; Wu 2004). Urban landscape heterogeneity should be expressed by structure–function boundaries rather than simple regular units. Urban landscape planning implemented for UHI mitigation also requires the rearrangement of not only the urban spatial landscape but also urban functions, and the research units should be closely linked to urban planning so that the results can be easily applied to policy formulation. To this end, Sun et al. (2013) and Yao et al. (2019) adopted the urban function zone (UFZ) as a special spatial unit for the study of UHI. The UFZ is directly combined with irregular urban blocks with specific socioeconomic activities, spatial characteristics, anthropogenic activity, and energy consumption, which thus function as the effective urban planning unit (Tian et al. 2010). Using the UFZ as the unit to study the UHI effect thus enables better conclusions to be drawn regarding urban planning to improve the urban thermal environment. However, there are still few studies that have tried to further investigate the interactions between urbanization and the UHI effect at the urban function scale. Therefore, there is an urgent need to identify appropriate urban landscape factors for characterizing the UHI effect under an urban functional framework that would be both ecologically meaningful and useful and intuitive to urban planners.

In view of this, a highly urbanized region in the city of Beijing, China, was selected as the study area to discuss the issues related to UHI effect. The study area was divided into >5000 UFZ blocks with different spatial forms, and the quantitative relationship between the seasonal LST and three types of urban landscape factors (surface biophysical parameters, building forms, and landscape pattern metrics) in these UFZ blocks were explored using two different spatial regression models, i.e., the ordinary least squares and the geographically weighted regression models. Specifically, the aims of this study were as follows: (1) to examine the potential spatiotemporal heterogeneity of the seasonal LST assigned UFZs and (2) to identify the potential heterogeneity in the urban landscape factors controlling the seasonal LST variations in different UFZs.

Materials and methodology

Study area

The city of Beijing is located on the Northern China Plain (39°26′~41°03′ N and 115°25′~117°30′ E), which belongs to a temperate continental monsoon climate with an average temperature of 12°C and distinct seasons (Wu et al. 2020a; Yao et al. 2020). As the capital city of China, Beijing has experienced rapid urbanization since the reform and opening-up policy (Peng et al. 2016). At present, Beijing has become a comprehensive metropolis with a dense population and diverse urban functions (Yao et al. 2019). Along with this, the UHI effect in the metropolitan region of Beijing has become increasingly significant. In this region, a nearly > 4 °C daily temperature gap has been reported by relevant studies (Sun et al. 2013). Coordinating the contradiction between sustainable urban health and thermal environmental regulation has thus become a great challenge for the local government. For this reason, we chose the urbanized region within the fifth ring road of Beijing (with an area of approximately 670km^2; Fig. 1) as the study region, which covers most of the central urban districts that have the highest rates of urbanization and the greatest population densities.

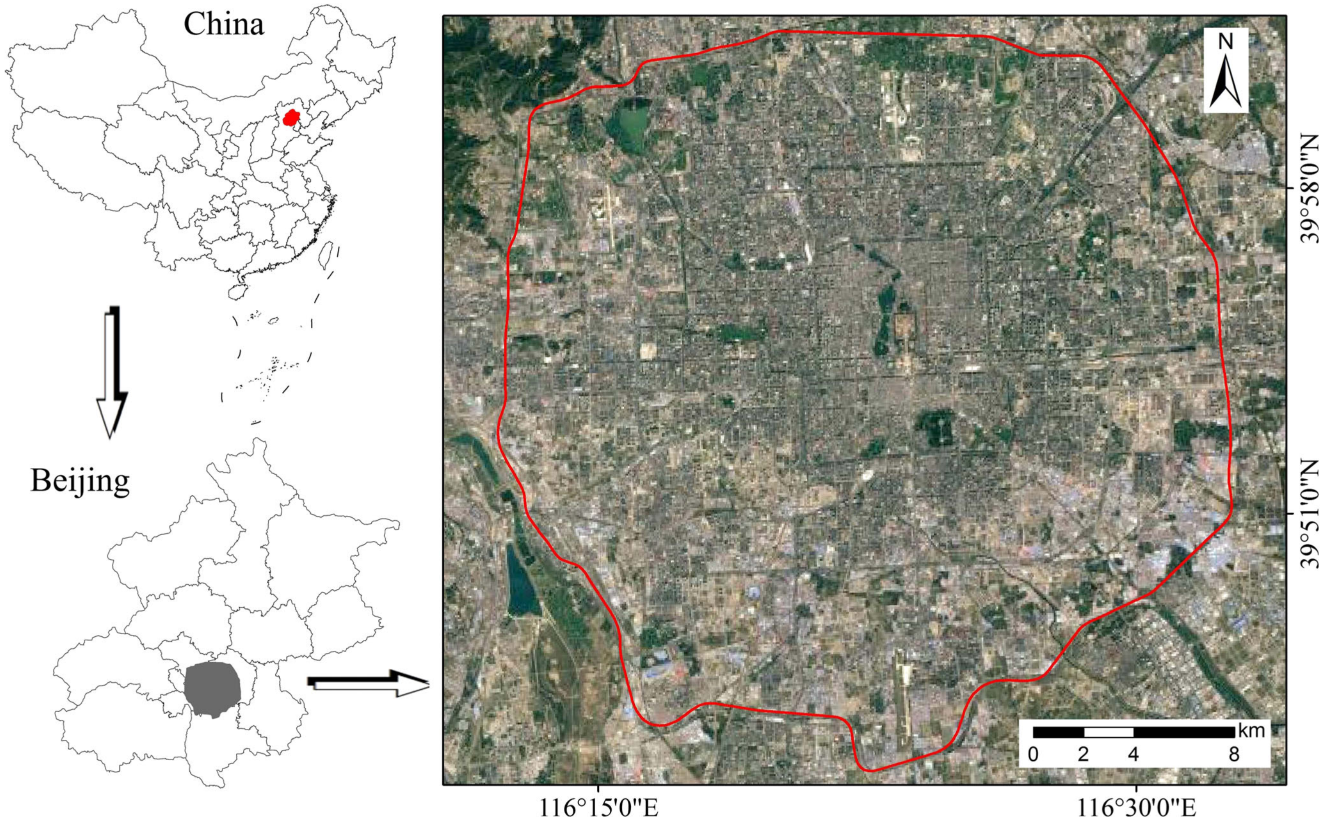

Fig. 1 Spatial location of the study area

Data collection and processing

Interpretation of land cover and UFZ

In this study, we used high-resolution (pan-sharped to 1×1 m) IKONOS imagery (cloud-free, acquired on 29 July 2012) to interpret the information related to the land cover and UFZs. An object-oriented classification method was applied to extract six types of land cover, i.e., built-up area, water body, farmland, forest, lawn, and bare land, as shown in Fig. 2. We validated the classification by ground-truthing images at approximately 400 random points. The overall accuracy of the classification was 85.8%, and the kappa coefficient was 0.75, indicating that the classification results were highly reliable (Yao et al. 2018).

The IKONOS imagery and land cover data were then used to identify UFZs. Some scholars believe that the urban landscape, such as urban streets, rivers, or greenbelts, function as thermal blocking corridors (Sun et al. 2013; Yao et al. 2019). Therefore, these linear landscapes were firstly used to divide the city blocks in the study area. Then, the urban functions assigned to these blocks were identified according to the attribute information acquired through a web survey. By following the detained standard proposed by Yao et al. (2015), a total of 5116 urban blocks were identified and delineated into 10 types of UFZs (Table 1 and Fig. 2), including high-density residential zone (HRZ), low-density residential zone, (LRZ), government zone (GOZ), industrial zone (INZ), commercial zone (COZ), recreational zone (REZ), preservation zone (PRZ), agricultural zone (AGZ), public service zone (PSZ), and development Zone (DEZ). Then, we selected six of the types of UFZs (HRZ, COZ, GOZ, PSZ, REZ, and INZ) for subsequent analysis, which occupied >90% of the study area. The land cover coverage in each type of UFZ is summarized and illustrated in Fig. 3, showing that built-up area, forest, and lawn were the major types in the selected types of UFZ for analysis.

Land surface temperature retrieval

Four radiometrically calibrated Landsat 8 imagery of the study area were collected from a geospatial data cloud platform provided by the Chinese Academy of Sciences (www.gscloud.cn) to retrieve the LST, acquired in spring (15 May 2014), summer (19 August 2014), autumn (6 October 2014), and winter (25 December 2014), respectively. By following the LST retrieval procedure presented by Li et al. (2020), the radiation equation algorithm was used to estimate the LST from the Landsat 8 data for the study area, and the results are shown in Fig. 4.

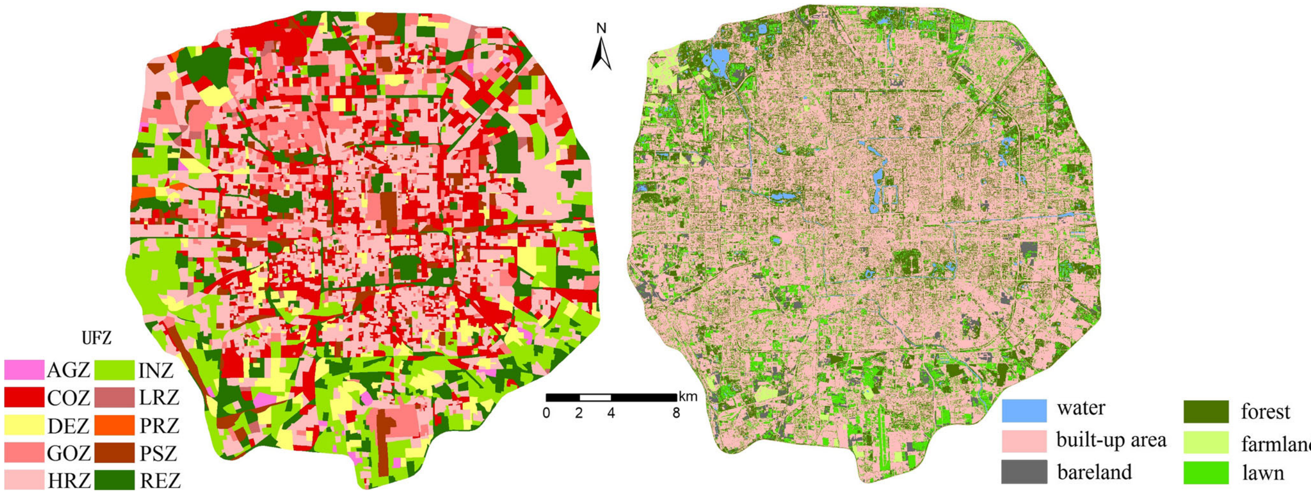

Fig. 2 The spatial details of the land cover and urban function zones of the study area. *UFZ* urban function zone, *AGZ* agricultural zone, *COZ* commercial zone, *DEZ* development zone, *GOZ* government zone, *HRZ* high-density residential zone, *INZ* industry zone, *LRZ* low-density residential zone, *PRZ* preservation zone, *PSZ* public service zone, *REZ* recreational zone

Urban landscape factor selection

By reviewing previous studies on the relationship between urban landscape factors and the UHI effect (Chen et al. 2012; Deilami et al. 2018; Wu and Ren 2018), this study selected three types of factors to explain the variations in the LST for the study area (Table 2), i.e., surface biophysical parameters, building forms, and landscape pattern metrics. All of these factors were calculated based on the UFZ blocks as the analysis units.

Surface biophysical parameters

Surface biophysical parameters can be treated as important ecological indicators for describing land surface features in urban regions. With the rapid development of remote sensing technology, surface biophysical factors have been widely used in UHI-related studies (Peng et al. 2018). In this paper, three types of surface biophysical parameters, including the normalized difference vegetation index (NDVI), the normalized difference built-up index (NDBI), and the modified normalized difference water index (MNDWI), characterizing urban green spaces, impervious surfaces, and water bodies, respectively, were chosen as the potential factors on the urban thermal environment variations. All three indices were obtained from remote sensing imagery (Landsat 8).

Building forms

Buildings are the most important landscape components in urban regions, which can directly disturb both the sensible and latent heat fluxes in urbanized regions (Kikegawa et al.

Table 1 Detailed interpretations of the urban function zones in the study area

UFZ	Area (km^2)	Description
High-density residential zone (HRZ)	213.73	High proportion of impermeable surfaces; a typical residential area in Beijing, consisting mainly of low- and high-rise buildings with a dense population
Low-density residential zone (LRZ)	3.71	Low proportion of impermeable surfaces; mainly for low-rise buildings with a sparse population
Government zone (GOZ)	63.58	Mainly government buildings, such as research institutes and campuses
Public service zone (PSZ)	37.54	Public areas serving the public, such as hospitals, libraries, and plazas
Industry zone (INZ)	89.94	Industrial sites of various natures, such as urban infrastructure and energy supply plants
Commercial zone (COZ)	118.79	Including city shopping malls, restaurants, hotels, and other public facilities
Recreational zone (REZ)	87.85	Urban parks, scenic spots, and other areas with a high green coverage
Preservation zone (PRZ)	1.76	Sites or relics, areas with natural or artificial green space, such as forest parks
Agricultural zone (AGZ)	4.76	Agricultural land, such as farmland and orchards
Development zone (DEZ)	45.17	The area under construction

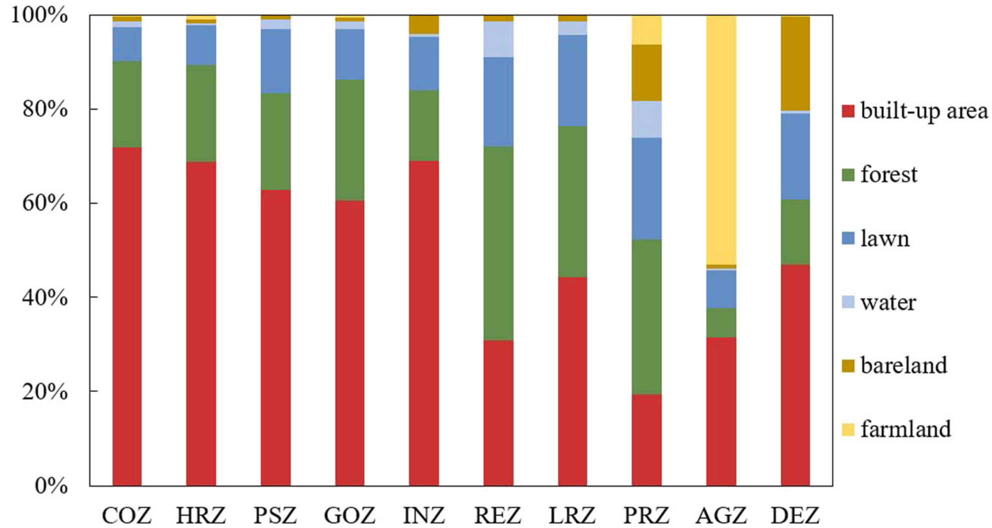

Fig. 3 The land cover compositions in each type of UFZ

2006). Previous studies have presented that both building area and geometry can significantly influence the scope and intensity of the UHI effect (Dai et al. 2018; Wang et al. 2019; Wu et al. 2020a). In this study, building height, building density, and building number were calculated to represent the characteristics of building forms and to examine their potential influence on the UHI effect. The building data in the study area were obtained from the open API of Baidu map (https://map.

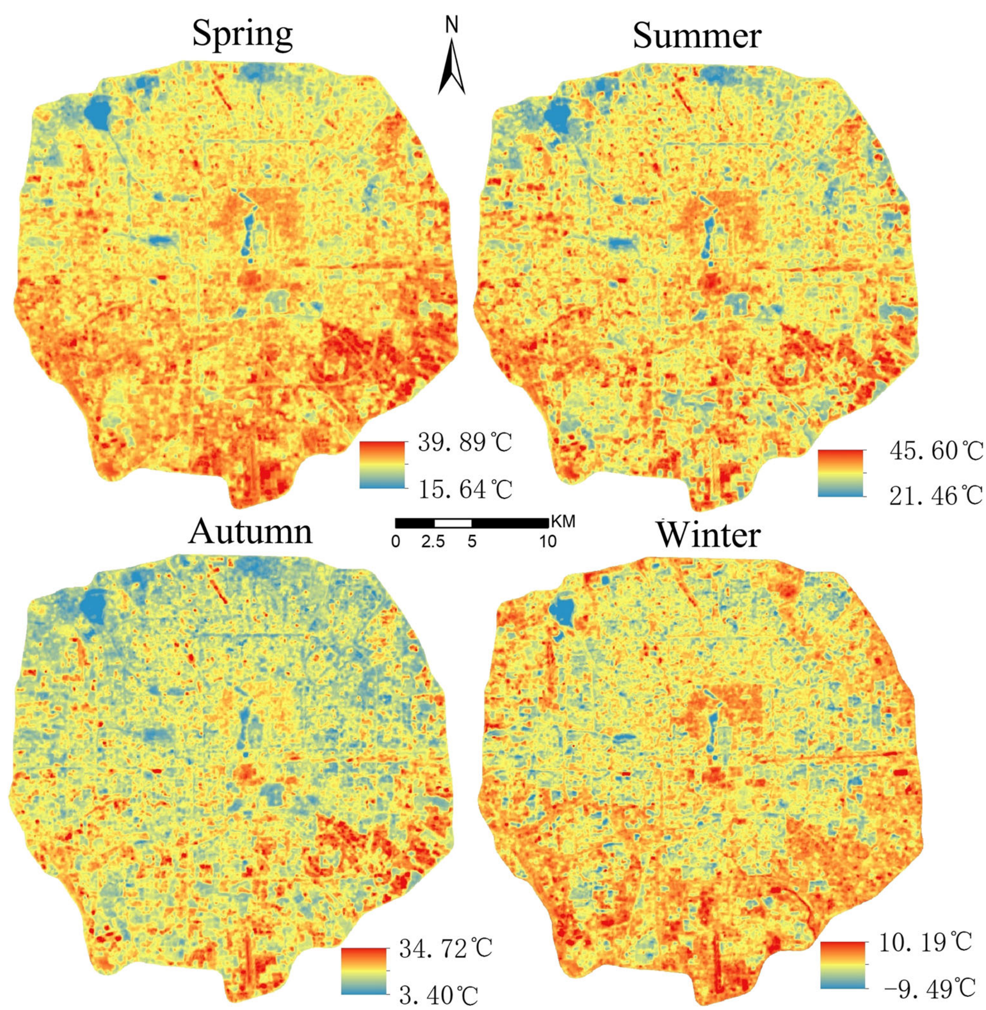

Fig. 4 The land surface temperature information in the four seasons of the study area

Table 2 Summary of the urban landscape factors used in this study

	Factor	Full name	Description	Unit	Formulae
Surface biophysical parameter	MNDWI	Modified normalized difference water index	Representing the general water status in the urban region	None	$MNDWI = \frac{band(green) - band(MIR)}{band(green) + band(MIR)}$
	NDBI	Normalized difference built-up index	Representing the general building status in the urban region	None	$NDBI = \frac{band(MIR) - band(NIR)}{band(MIR) + band(NIR)}$
	NDVI	Normalized difference vegetation index	Representing the general urban green space status in the urban region	None	$NDVI = \frac{band(NIR) - band(Red)}{band(NIR) + band(Red)}$
Building form	BN	Building number	The ratio of the number of buildings to the total area of the UFZ	$/km^2$	BN = sum of number / area of UFZ
	BD	Building density	The ratio of built-up area to the total area of the UFZ	km^2/km^2	BD = building area / area of UFZ
	BH	Building height	The average height of the buildings within the UFZ	m	BH = average height
Landscape pattern metric	PLAND	Percent landscape	Patches of area as a percentage of the entire landscape (at the class level)	%	$PLAND = P_i = \left(\sum_{j=1}^{n} \frac{a_{ij}}{A}\right)(100)$
	ED	Edge density	Shape complexity for a patch type or the landscape (at both the class and landscape levels)	m/ha	$ED = \frac{E}{A}$
	LSI	Landscape shape index	The total length of edge divided by the shortest possible edge length for the patch of area (at both the class and landscape levels)	None	$LSI = \frac{0.25E}{\sqrt{A}}$
	DIVISION	Landscape division index	Degree of separation of patch distribution in a landscape type (at both the class and landscape level)	%	$DIVISION = 1 - \sum_{j=1}^{n} \left(\frac{a_{ij}}{A}\right)^2$
	SHDI	Shannon's diversity index	To determine the extent to which one or more types of landscape structures dominate the landscape (at the class landscape level)	None	$SHDI = -\sum_{i=1}^{m} (P_i ln P_i)$

P_i the proportion of landscape patch type i, a_{ij} area (m^2) of land cover patch ij, A the area of UFZ block (m^2), E total length of patch boundary

Table 3 The rank results of the landscape factors by the random forest recursion feature elimination (RF-RFE) method

Landscape factor	Rank	Landscape factor	Rank
PLAND	1	CLUMPY	18
NLSI	2	PROX_AM	19
CONTIG_AM	3	SPLIT	20
DIVISION	4	CONNECT	21
GYRATE_AM	5	TE	22
LPI	6	SHAPE_MN	23
CA	7	CONTIG_MN	24
ED	8	PROX_MN	25
PD	9	PARA_AM	26
LSI	10	CIRCLE_AM	27
PARA_MN	11	SHAPE_AM	28
FRAC_AM	12	AREA_MN	29
CIRCLE_MN	13	IJI	30
MESH	14	AREA_AM	31
GYRATE_MN	15	AI	32
COHESION	16	NP	33
FRAC_MN	17	PLADJ	34

baidu.com/), including 230,769 building patches and corresponding attribute data.

Landscape pattern metrics

Urban landscape patterns are significantly related to biophysical factors and human activities. Landscape factors are thus often applied to detect and quantify their relationship with urban thermal complexities (Buyantuyev and Wu 2010; Hou and Estoque 2020). Due to the complexity and redundancy, however, the usage of landscape pattern metrics for ecological process analysis has been a controversial issue (Chen et al. 2016). In this study, a total of 34 landscape pattern metrics were calculated relating to the three major land cover types (built-up land, forests, and lawns) (Fig. 3). All of these factors with their full names/abbreviations are listed in Table S1. A cluster analysis was firstly conducted to group factors, in order to ensure the non-redundancy and representativeness of these factors (Fig. 5) (Chen et al. 2016). Then, the random forest recursion feature elimination (RF-RFE) method is a sequence backward selection algorithm based on the principle of maximum interval and was used to rank these metrics according to their relative importance (Table 3) and to select the metrics with most importance in each group (Qi et al. 2018).

Eventually, four types of landscape pattern metrics were determined, based on the above procedure, for subsequent analysis, i.e., landscape percentage (PLAND), edge density (ED), landscape shape index (LSI), and landscape division index (DIVISION). Shannon's diversity index (SHDI) is sensitive to the unbalanced distribution of various patch types in the landscape and can express the overall characteristics of the landscape within each UFZ, so it was also selected for the next analysis. The factors are as shown in Table 2.

Data analysis

The average LST values of all the seasons were calculated based on each analyzed UFZ block (Fig. 6), as the dependent factors. The spatiotemporal heterogeneity of the LST in the study area was discussed by applying spatial cluster analysis, i.e., global and local Moran's I analysis (Wang et al. 2020; Yao et al. 2019).

Then, the variance inflation factor (VIF) was used to detect the collinearity of independent variables. It was found that the VIF of all factors was less than 10, indicating poor multicollinearity among the independent variables. Finally, based on the calculated independent and dependent factors, we conducted further regression analysis in order to elaborate on the deeper quantitative relationship between urban landscape factors and seasonal LST. At present, the ordinary least squares (OLS) regression model is the most widely used global analysis method in UHI-related studies, to quantify the relationship between spatial and UHI variables (Deilami et al. 2018). The OLS regression model is shown as follows:

$$y = a_0 + a_1 x_1 + a_2 x_2 + \ldots + a_n x_n + \varepsilon \quad (1)$$

where a_0 is the regression constant; a_1, a_2, ..., a_n are the regression coefficients; y represents the average LST in UFZ blocks; x is the selected independent factors; and ε is the random error.

However, spatial heterogeneity exists objectively in almost the geological/ecological processes, and the UHI effect may show context sensitivity and vary significantly over time and space (Buyantuyev and Wu 2010). Therefore, the issue of spatial heterogeneity should be considered during parameter analysis and estimation. To address this, both OLS and geographically weighted regression (GWR) analysis were developed and compared to quantify the relationship between the selected urban spatial factors and seasonal LST assigned to different types of UFZs. As a model suitable for processing data with spatial heterogeneity, the GWR model can be expressed as follows:

$$y_i = \beta_0(u_i, v_i) + \sum_i^k \beta_k(u_i, v_i) x_{ik} + \varepsilon_i \quad (2)$$

where u_i and v_i are the latitude and longitude of sample i, respectively; β_0 and β_k are the regression coefficients with a weight of unity based on the Euclidean distance between samples; k refers to the number of variables; and ε_i is the random error.

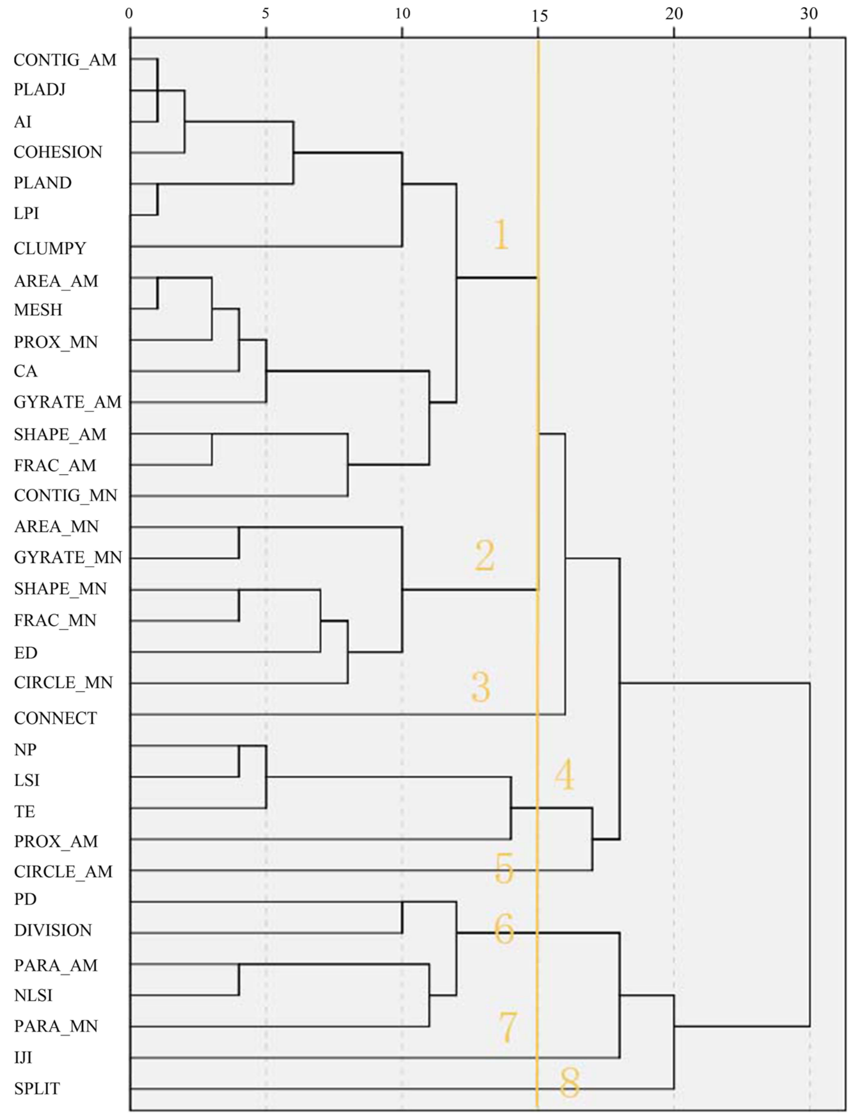

Fig. 5 Dendrogram of the cluster analysis for filtering of the landscape pattern metrics

We then selected the main factors responsible for the variations of LST and discussed the potential implications of these factors for urban landscape planning.

Results

The heterogeneous characteristics of LST in UFZs

The seasonal average LST information in each type of UFZ is shown in Fig. 7. Generally, all of the UFZs showed the highest average LST in the summer and the lowest in the winter. The INZ occupied the highest LST in all four seasons compared to the other types of UFZs, with an average LST gap of 1–3°C. In the spring, summer, and autumn seasons, the COZ showed the second highest average LST, while the REZ had the lowest average LST. The average LST differences among the PSZ, GOZ, and HRZ were small and largely statistically insignificant ($p > 0.05$) during all of the seasons. Specially, however, the REZ showed a relatively higher average LST than the other UFZs in addition to the INZ in winter.

Global Moran's I analysis for the seasonal UFZ LST of the study area was accomplished in the ArcGIS platform, with the I values of 0.431 (spring), 0.329 (summer), 0.392 (autumn), and 0.269 (winter). The positive results indicate that the LST had significant spatial clustering characteristics in all seasons ($p < 0.05$). The local Moran's I analysis further visualized the spatial agglomeration features of the UFZ LST, as shown in Fig. 8. The UFZ LST showed relatively fixed spatial agglomeration characteristics in all seasons, as the HH cluster was distributed in the southern region of the study area and the LL cluster in the north. In spring and autumn, both the HH and LL cluster regions were larger than those in the summer and winter seasons. By contrast, the lowest HH and LL cluster

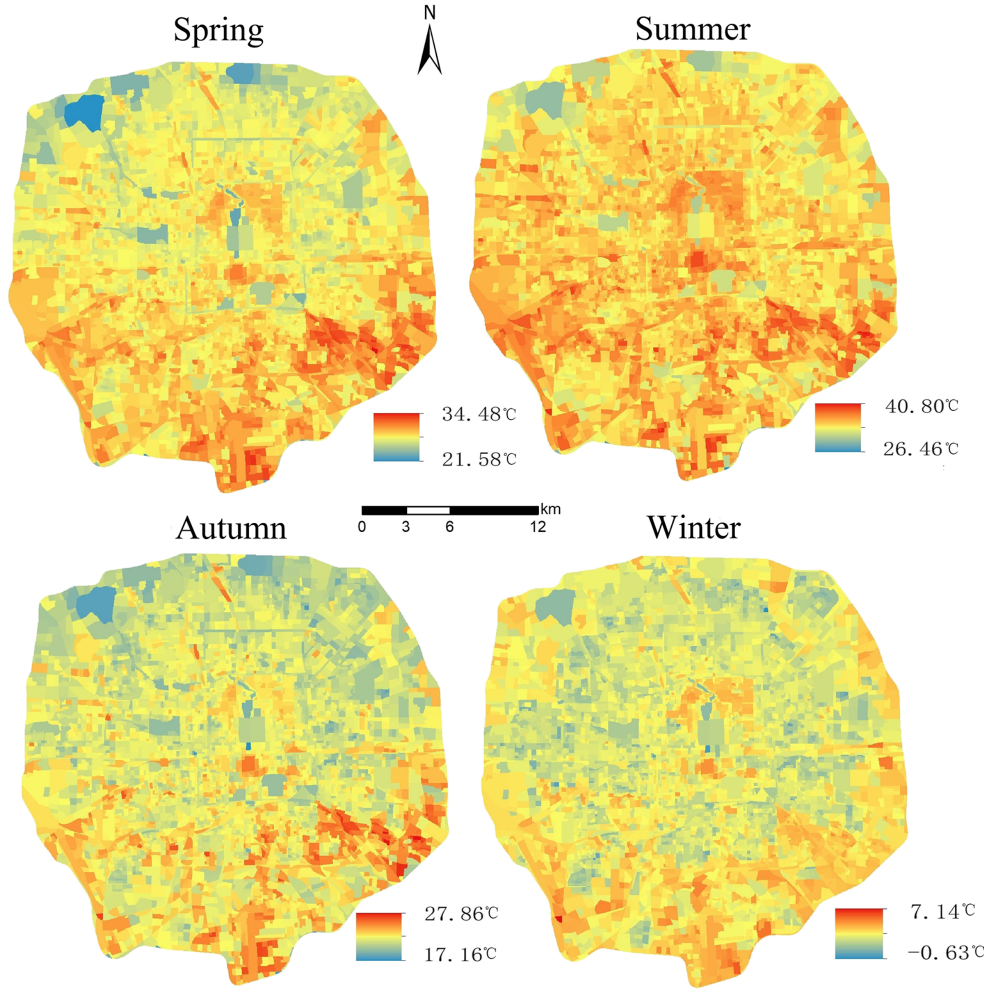

Fig. 6 The average land surface temperature (LST) in the UFZs of the four different seasons

coverage was found in summer and winter, respectively. Most of the UFZs of the study area were analyzed as insignificant areas of the LST clusters in summer and winter.

Effects of the urban spatial pattern on the heterogeneity of the LST

Comparison between the OLS and GWR models

In Table 4, the comparison results confirm that the GWR model showed better performance in predicting the relationship between the urban landscape factors and LST than that of OLS model, with higher adjust R^2 and lower *AICc* and *RSS* values during all seasons. In addition, the prediction residuals of the OLS and GWR models are illustrated in Fig. 9, to further support the regression performance. Most of the residual of GWR model fluctuates ranged between –1°C and 1°C in all seasons, and the average values of the residuals were all nearly equal to 0. In contrast, the residual of the OLS fluctuation range was significantly greater than that of the GWR in any season, with higher average residual values. This indicates that the GWR model, as the localized model with the premise of spatial heterogeneity, can better explain the spatial nonstationary of the seasonal LST and its influencing factors. Therefore, the GWR model was used in following analysis to explore the urban surface factors and LST variations.

Analysis results of the GWR model

The detailed GWR analysis results are shown in Fig. 10. The absolute value of the model coefficient for each factor represents the relative contribution importance for predicting the LST variation, where positive/negative values of the coefficient represent positive (+)/negative (–) relationships between urban landscape factors and the LST. In general, in all seasons, almost all of the independent factors except BN showed a significant contribution to the LST variations among all of the types of UFZs. The relative importance of these factors can be generally sorted in the order of surface biophysical factors > building forms > landscape factors. For different UFZs, the contribution directions (+/–) of the selected independent factors to the seasonal LST were similar, with their difference mainly reflected in the factors' contribution intensities along with different seasons.

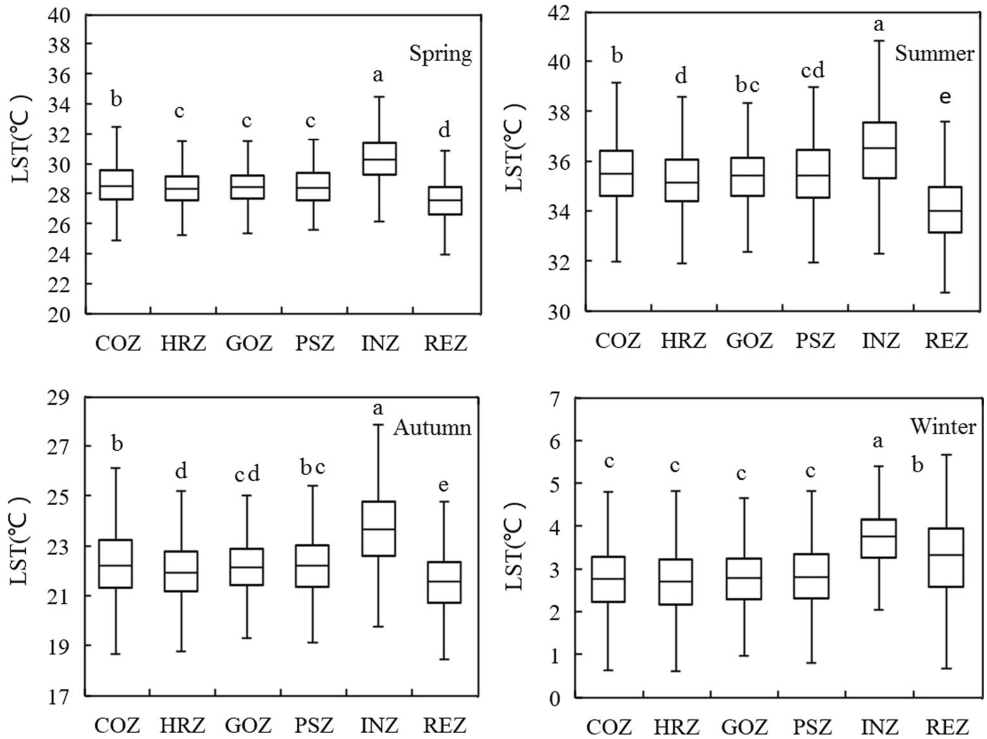

Fig. 7 The seasonal average LST for each type of UFZ. Different letters indicate significant difference in LST ($p < 0.05$)

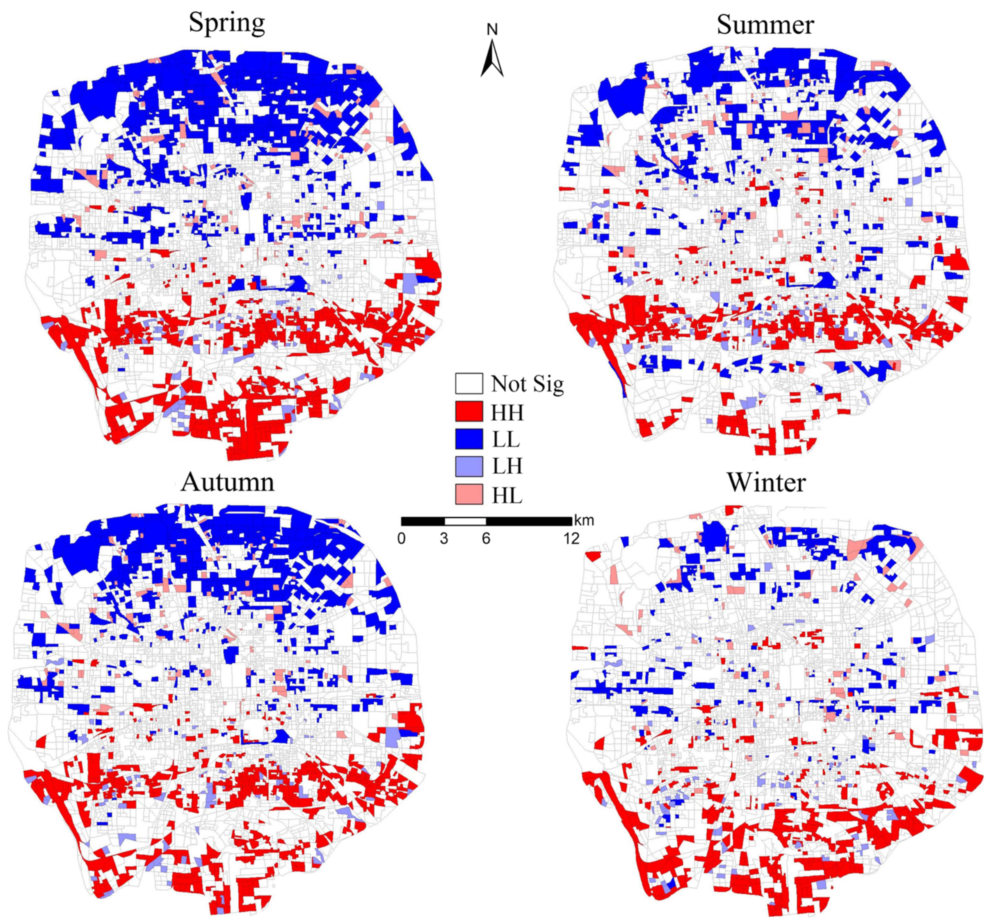

Fig. 8 LISA map for the average UFZ LST using local Moran's I analysis. HH indicates the spatial cluster with the higher LST; LL indicates the spatial cluster with the lower LST; the spatial outlier of the high LST value is displayed as HL, and that of the low LST value is mapped as LH. Not sig indicates that the spatial cluster is insignificant

In spring, the main effective factors were basically the same for all UFZs, except for the relative importance of PLAND_f/l being significantly higher in the REZ than in the other UFZs. NDBI (+) was the major contributor for all UFZs, while MNDWI (–) and NDVI (–) acted as the secondary contribution factors for the different UFZs (MNDWI for GOZ, INZ, and REZ; NDVI for the others). For all of the UFZs, BD (+), PLAND_b (+), SHDI (–), DIVISION_f/l (+) also performed as effective factors for influencing the LST.

In the summer, the main effective factors of each type of UFZ began to differ. NDBI (+) still contributed as the major contributors for all UFZs. However, the difference is that the contribution of the factors related to urban green space (forest and lawn) increased, such as NDVI (–), PLAND_f/l (–), and DIVISION_f/l (+). Among them, NDVI became the second most important factor impacting the LST variation for all UFZs.

In autumn, MNWI (–) became the major contribution factor rather than NDBI (+) for all UFZs except for the INZ. The relative importance of NDVI (–) in some UFZs went beyond NDBI, such as the COZ, HRZ, PSZ, and REZ. Meanwhile, the relative contribution of building-related factors increased significantly, such as BD and PLAND_b.

In winter, the factors' contribution intensities differed significantly to those of the other seasons. MNWI (–) contributed as the major contribution factors, while both NDBI and NDVI acted as positive contributors to the LST. The other types of factors showed relatively lower contributions to the LST than those in the other seasons.

Discussion

The spatiotemporal heterogeneity in urban thermal environments

This study enabled us to realize the high degree of heterogeneity in urban thermal environments. From a spatial perspective, the whole study area showed a general "working–living–resting" thermal gradient (Fig. 7). However, the seasonal LST varied significantly in both the spatial and temporal dimensions, due to the disorderly spatial layout and the high diversity of urban land surface characteristics of the UFZs (Sun et al. 2013; Yao et al. 2020). There were a large number of UFZ blocks with high temperature clustered around the southern part of the study area, which were mostly in the INZ (Figs. 2 and 8). However, the UFZ blocks with low temperature, e.g., the REZ, were mainly clustered around the northern part of the study area, which was spatially isolated from the regions under higher thermal pressure. The imbalanced distribution of such patches would further cause a significant segregation of urban thermal environments (Wu et al. 2020b). From a temporal perspective, according to the results of the global Moran's I analysis, more significant spatial heterogeneity of the LST was found in the seasons of spring and autumn (with relatively mild

Table 4 Comparison of the regression model performance between the ordinary least squares (OLS) and geographically weighted regression (GWR) methods. The adjusted coefficient of determination (adjust R^2), the Akaike Information Criterion (*AICc*), and the residual sum of squares (*RSS*) were used to evaluate the performances of the built models, and higher adjust R^2 and lower *AICc* and *RSS* values indicate better model performance (Mitchel 2005; Wang et al. 2020)

		Adjust R^2	*AICc*	*RSS*
Spring	OLS	0.73	10914.38	2864.68
	GWR	0.84	9117.12	1399.64
Summer	OLS	0.68	11152.86	3017.35
	GWR	0.77	10095.79	1777.90
Autumn	OLS	0.60	12148.47	3747.71
	GWR	0.74	10572.93	2054.41
Winter	OLS	0.55	8011.58	1522.65
	GWR	0.71	6562.71	804.97

climatic background condition) rather than that in summer and winter. Lower spatial heterogeneity, especially in summer, means that the entire urban area has a relative homogeneous high temperature, indicating a strong UHI effect of the study area (Dai et al. 2018; Quan et al. 2014).

Factors responsible for the seasonal LST

This study examined the relationship between seasonal LST and urban landscape factors from the perspective of UFZ, and the results revealed the dominant factors for the spatial variability in the seasonal LST of the study area.

Generally, all three types of factors were found to have significant influence on the variation of the LST. By comparison, the surface biophysical factors acted as the major contributors for all the seasons, including NDBI, NDVI, and MNDWI. The three types of indices have been widely used to characterize urban buildings, urban green space, and water body features that contain rich land cover spectral information (Estoque et al. 2017; Peng et al. 2018). This indicates that, in all seasons, the factors that characterized artificial buildings, green spaces, or water bodies were always the most powerful in affecting LST variations. Previous studies have identified the above land cover types as the source and sink landscape of urban thermal risk, respectively (Kong et al. 2014; Sun et al. 2018). Moreover, the building forms and landscape factors also showed strong ability to explain the variation of the LST, but with lower interpretation rates than that of surface biophysical factors. This is consistent with the findings by Peng et al. (2018), Yao et al. (2020), and Zhou et al. (2011); namely, the most effective way to alter the urban thermal environment is to simply change the landscape structure (e.g., increasing urban green coverage) rather than altering their pattern or layout.

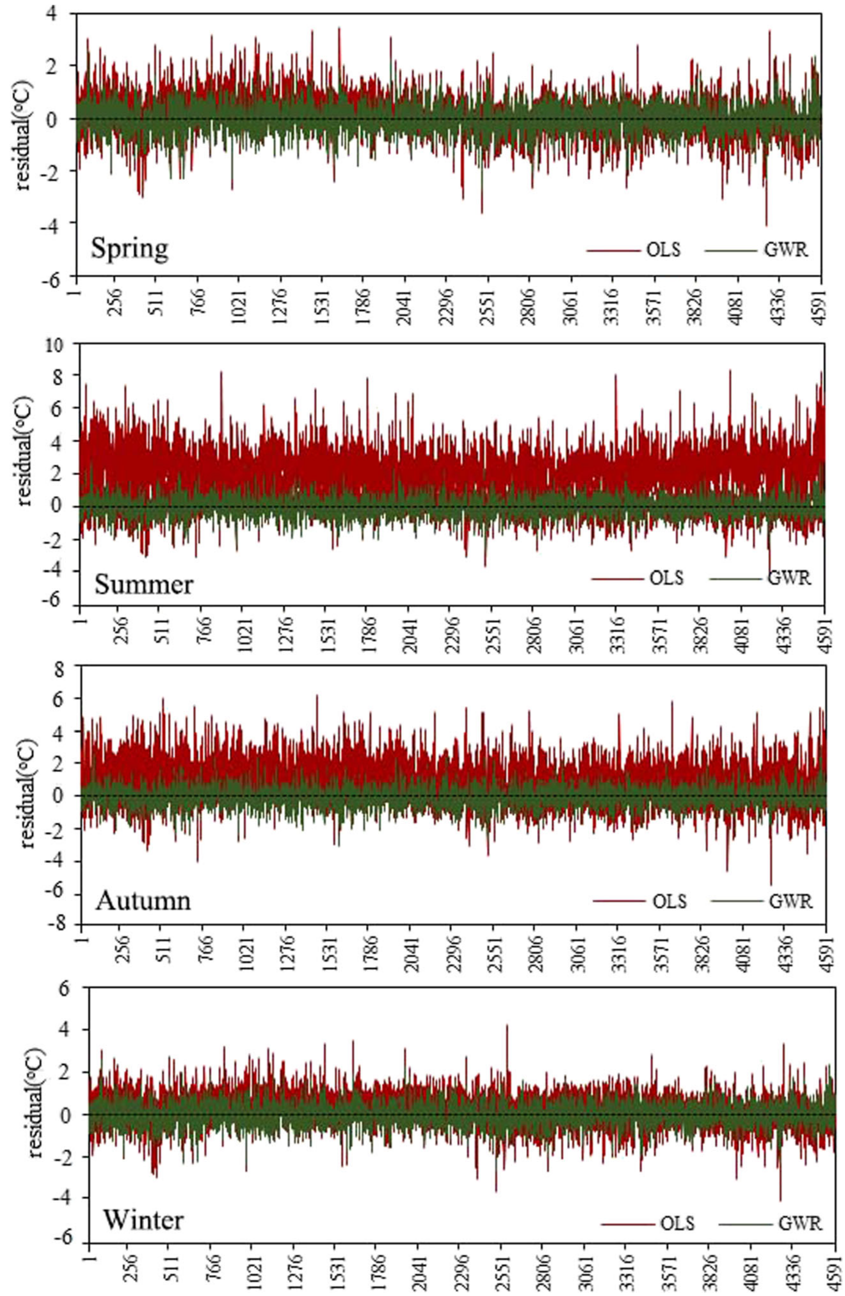

Fig. 9 The residual fluctuation on predicting the seasonal LST by the OLS and GWR models. The *x*-axis represents each UFZ block for analysis

Moreover, the factors affecting LST showed different phenomena in different seasons. Artificial surfaces are the main type of landscape in the study area, which are reported to be closely related to urban thermal exchange process (Kuang et al. 2015; Li et al. 2011). Building-related factors showed a significant relationship with seasonal LST. More buildings signify higher NDBI and PLAND_b and lower BD and would thus strongly intensify the UHI effect. However, the growth status and coverage of urban green space changed obviously in different seasons (Yao et al. 2020). As one of the most important sink landscapes for UHI mitigation, the role of urban green space in the LST would vary or even reverse under different climate conditions, as shown in Fig. 10. For example, in winter, after deciduous urban forest and lawn lose their leaves due to the cold weather, the exposed soil beneath the vegetation canopy shows similar thermal inertia characteristics to non-vegetated landscapes, such as buildings (Kikegawa et al. 2006; Morabito et al. 2016). By the same token, in summer or autumn, urban green spaces reach their optimal growth and largest canopy, with the latent heat flux capacities by canopy evapotranspiration along with the shedding of leaves benefiting the thermal exchange ability and thus presenting a cooling effect for urban thermal environments (Sun and Chen 2017; Yao et al. 2020). This explains the seasonal fluctuation of vegetation-related parameters in predicting the LST in different seasons.

Spring	COZ	HRZ	PSZ	GOZ	INZ	REZ
MNDWI	-1.252	-0.387	-0.666	-1.833	-9.225	-5.61
NDBI	24.93	25.777	25.642	26.05	35.813	20.216
NDVI	-3.446	-2.855	-1.626	-0.45	-4.193	-2.145
BN	-	-	-	-	-	-
BD	1.343	1.447	1.282	1.234	1.908	1.187
BH	-0.036	-0.038	-0.037	-0.037	-0.054	-0.043
PLAND_b	1.031	1.028	1.039	1.034	2.004	0.018
PLAND_f	-0.544	-0.441	-0.449	-0.442	-0.115	-1.332
PLAND_l	-0.045	-0.043	-0.054	-0.052	-0.305	-1.034
ED_b	-0.001	-	-0.002	-0.001	0.002	0.001
ED__f	-0.001	-0.001	-0.002	-0.002	0.001	-
ED__l	-0.002	-0.002	-0.003	-0.003	0.001	-0.001
LSI_b	-0.113	-0.107	-0.108	-0.13	-0.108	-0.121
LSI_f	-0.092	-0.09	-0.096	-0.101	-0.078	-0.083
LSI_l	-0.046	-0.045	-0.057	-0.037	-0.009	-0.025
DIVISION_b	-0.1	-0.097	-0.111	-0.259	-0.279	-0.259
DIVISION_f	0.334	0.234	0.266	0.225	0.381	0.473
DIVISION_l	0.207	0.255	0.267	0.33	0.365	0.44
ED	0.002	0.002	0.004	0.003	-0.004	-
LSI	0.039	0.032	0.037	0.032	-0.005	0.029
DIVISION	-0.053	-0.058	-0.004	-0.03	-0.014	-0.042
SHDI	-0.628	-0.562	-0.702	-0.729	-0.494	-0.535

Summer	COZ	HRZ	PSZ	GOZ	INZ	REZ
MNDWI	-3.909	-3.928	-1.704	-1.193	-3.077	-1.201
NDBI	7.836	8.1	10.556	13.212	16.524	7.108
NDVI	-7.463	-7.729	-5.815	-2.114	-2.696	-3.316
BN	–	–	–	–	–	–
BD	1.062	1.121	0.833	0.873	2.054	1.289
BH	-0.041	-0.043	-0.043	-0.043	-0.057	-0.048
PLAND_b	1.039	1.037	1.046	0.841	2.007	0.025
PLAND_f	-1.037	-1.034	-0.644	-1.035	-0.211	-1.025
PLAND_l	-0.353	-0.047	-0.063	-0.059	-1.003	-0.932
ED_b	-0.002	-0.001	-0.002	-0.002	0.001	–
ED__f	-0.002	-0.001	-0.002	-0.002	0.001	–
ED__l	-0.003	-0.002	-0.003	-0.003	0.002	-0.001
LSI_b	-0.038	-0.037	-0.047	-0.068	-0.016	-0.051
LSI_f	-0.101	-0.098	-0.103	-0.114	-0.092	-0.093
LSI_l	-0.045	-0.046	-0.054	-0.031	-0.024	-0.033
DIVISION_b	-0.095	-0.125	-0.109	-0.048	-0.11	-0.075
DIVISION_f	0.714	0.658	0.778	0.579	0.628	1.194
DIVISION_l	0.345	0.159	0.242	0.02	0.45	0.592
ED	0.003	0.002	0.004	0.004	-0.003	–
LSI	-0.055	-0.053	-0.04	-0.06	-0.109	-0.052
DIVISION	-0.083	-0.076	-0.024	-0.063	-0.047	-0.06
SHDI	-0.493	-0.297	-0.525	-0.598	-0.024	-0.19

Autumn	COZ	HRZ	PSZ	GOZ	INZ	REZ
MNDWI	-12.394	-11.598	-11.511	-9.364	-5.675	-7.916
NDBI	1.452	2.484	1.975	4.023	8.873	1.05
NDVI	-4.736	-4.335	-4.068	-1.038	-1.304	-1.87
BN	–	–	–	–	–	–
BD	1.543	1.664	1.181	1.204	2.989	1.875
BH	-0.038	-0.041	-0.039	-0.04	-0.06	-0.048
PLAND_b	1.032	1.132	1.037	1.032	2.013	0.026
PLAND_f	-0.465	-0.496	-0.596	-0.459	-0.09	-1.002
PLAND_l	-0.047	-0.042	-0.058	-0.052	-0.209	-0.031
ED_b	-0.002	-0.002	-0.003	-0.002	-0.001	-0.001
ED__f	-0.001	-0.001	-0.002	-0.002	–	-0.001
ED__l	-0.004	-0.003	-0.004	-0.004	-0.001	-0.002
LSI_b	-0.006	-0.012	-0.015	-0.04	-0.042	-0.046
LSI_f	-0.087	-0.083	-0.092	-0.101	-0.06	-0.071
LSI_l	-0.032	-0.038	-0.042	-0.024	-0.03	-0.029
DIVISION_b	-0.016	-0.032	-0.022	-0.074	-0.146	-0.006
DIVISION_f	0.025	0.026	0.029	0.022	0.016	0.022
DIVISION_l	0.135	0.111	0.148	0.55	0.298	0.07
ED	0.004	0.003	0.004	0.004	0	0.002
LSI	-0.077	-0.06	-0.068	-0.074	-0.018	-0.022
DIVISION	-0.13	-0.117	-0.061	-0.1	-0.108	-0.103
SHDI	-0.139	0.019	-0.186	-0.229	0.248	0.145

Winter	COZ	HRZ	PSZ	GOZ	INZ	REZ
MNDWI	-35.531	-34.765	-30.084	-30.849	-36.546	-33.905
NDBI	34.342	32.795	26.542	29.109	31.503	30.706
NDVI	20.153	20.333	15.756	15.839	25.478	21.406
BN	–	–	–	–	–	–
BD	1.004	1.041	0.948	0.861	1.284	0.475
BH	-0.007	-0.009	-0.009	-0.009	-0.02	-0.013
PLAND_b	0.318	0.317	0.322	0.32	0.304	0.108
PLAND_f	0.022	0.021	0.026	0.023	0.009	0.218
PLAND_l	0.019	0.016	0.023	0.022	0.001	0.014
ED_b	-0.002	-0.002	-0.003	-0.002	–	-0.001
ED__f	-0.002	-0.002	-0.002	-0.002	–	-0.001
ED__l	-0.003	-0.003	-0.003	-0.003	-0.001	-0.002
LSI_b	0.01	0.017	0.02	0.031	0.023	0.04
LSI_f	0.026	0.019	0.033	0.038	0.006	0.003
LSI_l	0.017	0.023	0.031	0.022	0.011	0.017
DIVISION_b	-0.115	-0.178	0.009	-0.03	-0.435	-0.294
DIVISION_f	0.238	0.134	0.143	0.258	0.296	0.21
DIVISION_l	0.285	0.259	0.125	0.125	-0.245	0.267
ED	0.004	0.004	0.005	0.005	0	0.002
LSI	0.005	0.03	0.02	0.012	0.06	0.071
DIVISION	0.005	0.009	0.039	0.013	0.054	0.028
SHDI	-0.121	-0.023	-0.373	-0.273	0.331	0.046

Fig. 10 The contribution coefficients of the urban landscape factors to the seasonal LST of different UFZs by GWR analysis. b, f, and l indicate built-up area, forest, and lawn for landscape analysis at the class level; the length of the color strip indicates the relative contribution of a specific factor; – represents a value less than 0.001

When focusing on the UFZ perspective, the similarities and differences in the key factors of the LST among different UFZs are partly due to the above climate reasons and partly due to their urban functional activities and landscape features. With relatively high built-up coverage and intensive producing activities, the building-related factors (e.g., NDBI, BD, and PLAND_b) contributed as more important factors than urban greening factors, even in the autumn when NDVI performed as a better predictor of the LST than NDBI in the other UFZs (Fig. 10). The COZ, PSZ, GOZ, and HRZ had similar LSTs and key influence factors for all seasons. This can be explained by the similar intensities of the production activities and the landscape compositions and building forms in these UFZs (Li et al. 2020; Wu et al. 2020a). For the REZ, the main difference to the other UFZs lies in the factor sensitivity related to urban green spaces, i.e., DIVISION_f/l (+). In the summer, with the strongest UHI intensity, it is essential to develop large urban green parks with scale advantage rather than discrete green patches to benefit urban thermal risk regulation (Chen et al. 2014b).

Implications of this study

This study highlighted the significant role of urban landscape factors on controlling an urban thermal environment at the urban function scale. The results related to surface biophysical parameters, building forms, and landscape pattern metrics can provide important insights on the impact of urbanization on the UHI effect being mitigated by urban landscape optimization.

However, urban thermal regulation tasks should consider the climate background and spatial planning unit. Peng et al.

(2018) conducted a case study under subtropical marine monsoon climate conditions and found that NDVI retained a strong contribution to the LST variation throughout the whole year, because of the local climate conditions of evergreen vegetation. This study adopted irregular UFZ blocks as spatial units for analysis, which is different from most previous studies (Deilami et al. 2018). The whole study area presented a significant urban thermal gradient assigned to different types of UFZs. Due to different urban function activities and landscape heterogeneity (Yao et al. 2019; Yu et al. 2021), the major responsible factors of different UFZs varied with the types and contribution intensities (Fig. 10). To mitigate a high thermal environment of a given UFZ, it would thus be appropriate to focus on specific landscape elements of said UFZ as a suitable reference target. Furthermore, scholars have examined the effectiveness of various landscape factors on predicting the urban LST at different spatial scales and concluded that these landscape factors may not often provide the same performance in explaining LSTs (Chen et al. 2014a; Hamstead et al. 2016; Zhou et al. 2014). This may also explain why the landscape composition factors (surface biophysical parameters) contributed much more than pattern factors (building forms and landscape pattern metrics) in our study. However, in the face of urban land contradiction (Kikegawa et al. 2006), optimizing the spatial configuration (e.g., BH or SHDI) of the existing urban landscape is a more cost-effective solution for alleviating urban thermal stress.

Conclusion

Understanding the impact of urban landscape heterogeneity on the UHI effect is of great significance for urban thermal regulation. In this study, surface biophysical parameters, building form, and landscape pattern metrics were selected to depict the urban landscape characteristics. The relationship between the seasonal LST and the selected urban landscape factors was discussed from the perspective of UFZ in the metropolitan region of Beijing. The main findings can be summarized as follows: (1) Significant spatiotemporal heterogeneity of the LST was found in the study area, and there was an obvious temperature gradient assigned to the UFZs. (2) All types of landscape factors showed a significant contribution to seasonal LST, in the order of surface biophysical factors > building forms > landscape factors; however, their contributions varied in different seasons. (3) The major contributing factors showed a certain difference due to the diversity of the urban functions and landscape structures in the study area. This study expands the understanding on the complex relationships among urban landscape, function, and thermal environment, which could benefit urban landscape planning for UHI alleviation.

Supplementary Information The online version contains supplementary material available at https://doi.org/10.1007/s11356-021-13695-y.

Acknowledgements We would sincerely thank the editors and anonymous reviewers, for their valuable advices regarding this manuscript.

Author contribution Conceptualization: Lei Yao and Tong Li Methodology: Tong Li Software: Tong Li Formal analysis: Tong Li and Ying Xu Writing—original draft: Tong Li Writing—review and editing: Lei Yao Supervision: Lei Yao and Ying Xu Funding acquisition: Lei Yao and Ying Xu Resources: Lei Yao

All authors have read and agreed to the published version of the manuscript.

Funding This study was financed by the National Natural Science Foundation of China (41701206), the Humanities and Social Science Foundation of Ministry of Education of China (20YJCZH198), the Natural Science Foundation of Shandong Province, China (ZR2017BD011), and the China Postdoctoral Science Foundation (2017M622256).

Availability of data and materials The data presented in this study are available on request from the corresponding author. The data are not publicly available due to the privacy agreement among co-authors.

Declarations

Ethical approval This manuscript has not been published elsewhere in part or in entirety.

Consent to participate and publish All the authors contributed materially to this study, have reviewed and approved the manuscript, and agree with submission and publication to the journal.

Competing interests The authors declare no competing interests.

References

Arnfield AJ (2003) Two decades of urban climate research: a review of turbulence, exchanges of energy and water, and the urban heat island. Int J Climatol 23:1–26

Buyantuyev A, Wu J (2010) Urban heat islands and landscape heterogeneity: linking spatiotemporal variations in surface temperatures to land-cover and socioeconomic patterns. Landsc Ecol 25:17–33

Chen A, Sun R, Chen L (2012) Studies on urban heat island from a landscape pattern view: a review. Acta Ecol Sin 32:4553–4565

Chen A, Yao L, Sun R, Chen L (2014a) How many metrics are required to identify the effects of the landscape pattern on land surface temperature? Ecol Indic 45:424–433

Chen A, Yao XA, Sun R, Chen L (2014b) Effect of urban green patterns on surface urban cool islands and its seasonal variations. Urban For Urban Green 13:646–654

Chen A, Zhao X, Yao L, Chen L (2016) Application of a new integrated landscape index to predict potential urban heat islands. Ecol Indic 69:828–835

Dai Z, Guldmann J-M, Hu Y (2018) Spatial regression models of park and land-use impacts on the urban heat island in central Beijing. Sci Total Environ 626:1136–1147

Deilami K, Kamruzzaman M, Liu Y (2018) Urban heat island effect: a systematic review of spatio-temporal factors, data, methods, and mitigation measures. Int J Appl Earth Obs Geoinf 67:30–42

Estoque RC, Murayama Y, Myint SW (2017) Effects of landscape composition and pattern on land surface temperature: an urban heat island study in the megacities of Southeast Asia. Sci Total Environ 577:349–359

Gago EJ, Roldan J, Pacheco-Torres R, Ordóñez J (2013) The city and urban heat islands: a review of strategies to mitigate adverse effects. Renew Sust Energ Rev 25:749–758

Grimm NB, Foster D, Groffman P, Grove JM, Hopkinson CS, Nadelhoffer KJ, Pataki DE, Peters DPC (2008) The changing landscape: ecosystem responses to urbanization and pollution across climatic and societal gradients. Front Ecol Environ 6:264–272

Hamstead ZA, Kremer P, Larondelle N, McPhearson T, Haase D (2016) Classification of the heterogeneous structure of urban landscapes (STURLA) as an indicator of landscape function applied to surface temperature in New York City. Ecol Indic 70:574–585

Hou H, Estoque RC (2020) Detecting cooling effect of landscape from composition and configuration: an urban heat island study on Hangzhou. Urban For Urban Green 53:126719

Kedron PJ, Frazier AE, Ovando-Montejo GA, Wang J (2018) Surface metrics for landscape ecology: a comparison of landscape models across ecoregions and scales. Landsc Ecol 33:1489–1504

Kikegawa Y, Genchi Y, Kondo H, Hanaki K (2006) Impacts of city-block-scale countermeasures against urban heat-island phenomena upon a building's energy-consumption for air-conditioning. Appl Energy 83:649–668

Kong F, Yin H, James P, Hutyra LR, He HS (2014) Effects of spatial pattern of greenspace on urban cooling in a large metropolitan area of eastern China. Landsc Urban Plan 128:35–47

Kuang W, Liu Y, Dou Y, Chi W, Chen G, Gao C, Yang T, Liu J, Zhang R (2015) What are hot and what are not in an urban landscape: quantifying and explaining the land surface temperature pattern in Beijing, China. Landsc Ecol 30:357–373

Li J, Song C, Cao L, Zhu F, Meng X, Wu J (2011) Impacts of landscape structure on surface urban heat islands: a case study of Shanghai, China. Remote Sens Environ 115:3249–3263

Li X, Zhou W, Ouyang Z, Xu W, Zheng H (2012) Spatial pattern of greenspace affects land surface temperature: evidence from the heavily urbanized Beijing metropolitan area, China. Landsc Ecol 27:887–898

Li W, Cao Q, Lang K, Wu J (2017) Linking potential heat source and sink to urban heat island: Heterogeneous effects of landscape pattern on land surface temperature. Sci Total Environ 586:457–465

Li T, Cao JF, Xu MX, Wu QY, Yao L (2020) The influence of urban spatial pattern on land surface temperature for different functional zones. Landsc Ecol Eng 16:249–262

Mitchel A (2005) The ESRI Guide to GIS analysis. Esri Guide to Gis Analysis, 2. Esri Press

Morabito M, Crisci A, Messeri A, Orlandini S, Raschi A, Maracchi G, Munafò M (2016) The impact of built-up surfaces on land surface temperatures in Italian urban areas. Sci Total Environ 551–552:317–326

Peng J, Xie P, Liu Y, Ma J (2016) Urban thermal environment dynamics and associated landscape pattern factors: a case study in the Beijing metropolitan region. Remote Sens Environ 173:145–155

Peng J, Jia J, Liu Y, Li H, Wu J (2018) Seasonal contrast of the dominant factors for spatial distribution of land surface temperature in urban areas. Remote Sens Environ 215:255–267

Qi C, Zhaopeng M, Xinyi L, Qianguo J, Ran S (2018) Decision variants for the automatic determination of optimal feature subset in RF-RFE. Genes 9:301

Quan J, Chen Y, Zhan W, Wang J, Voogt J, Wang M (2014) Multi-temporal trajectory of the urban heat island centroid in Beijing, China based on a Gaussian volume model. Remote Sens Environ 149:33–46

Sun R, Chen L (2017) Effects of green space dynamics on urban heat islands: mitigation and diversification. Ecosyst Serv 23:38–46

Sun R, Lü Y, Chen L, Yang L, Chen A (2013) Assessing the stability of annual temperatures for different urban functional zones. Build Environ 65:90–98

Sun R, Xie W, Chen L (2018) A landscape connectivity model to quantify contributions of heat sources and sinks in urban regions. Landsc Urban Plan 178:43–50

Tian GJ, Wu JG, Yang ZF (2010) Spatial pattern of urban functions in the Beijing metropolitan region. Habitat Int 34:249–255

Ulpiani G (2021) On the linkage between urban heat island and urban pollution island: three-decade literature review towards a conceptual framework. Sci Total Environ 751:141727

Wang H, He Q, Liu X, Zhuang Y, Hong S (2012) Global urbanization research from 1991 to 2009: a systematic research review. Landsc Urban Plan 104:299–309

Wang X, Zhou T, Tao F, Zang FY (2019) Correlation analysis between UBD and LST in Hefei, China, using Luojia1-01 night-time light imagery. Appl Sci 9:20

Wang Y, Xu M, Li J, Jiang N, Wang D, Yao L, Xu Y (2020) The gradient effect on the relationship between the underlying factor and land surface temperature in large urbanized region. Land 10:20

Weng Q (2009) Thermal infrared remote sensing for urban climate and environmental studies: methods, applications, and trends. ISPRS J Photogramm Remote Sens 64:335–344

Wu J (2004) Effects of changing scale on landscape pattern analysis: scaling relations. Landsc Ecol 19:125–138

Wu Z, Ren Y (2018) A bibliometric review of past trends and future prospects in urban heat island research from 1990 to 2017. Environ Rev 27:241–251

Wu Z, Yao L, Ren Y (2020a) Characterizing the spatial heterogeneity and controlling factors of land surface temperature clusters: a case study in Beijing. Build Environ 169:106598

Wu Z, Yao L, Zhuang M, Ren Y (2020b) Detecting factors controlling spatial patterns in urban land surface temperatures: a case study of Beijing. Sustain Cities Soc 63:102454

Yang F, Qian F, Lau SSY (2013) Urban form and density as indicators for summertime outdoor ventilation potential: a case study on high-rise housing in Shanghai. Build Environ 70:122–137

Yao L, Chen L, Wei W, Sun R (2015) Potential reduction in urban runoff by green spaces in Beijing: a scenario analysis. Urban For Urban Green 14:300–308

Yao L, Wei W, Yu Y, Xiao J, Chen L (2018) Rainfall-runoff risk characteristics of urban function zones in Beijing using the SCS-CN model. J Geogr Sci 28:656–668

Yao L, Xu Y, Zhang B (2019) Effect of urban function and landscape structure on the urban heat island phenomenon in Beijing, China. Landsc Ecol Eng 15:379–390

Yao L, Li T, Xu M, Xu Y (2020) How the landscape features of urban green space impact seasonal land surface temperatures at a city-

block-scale: an urban heat island study in Beijing, China. Urban For Urban Green 52:126704
Yu Z, Jing Y, Yang G, Sun R (2021) A new urban functional zone-based climate zoning system for urban temperature study. Remote Sens 13:251
Zhou W, Huang G, Cadenasso ML (2011) Does spatial configuration matter? Understanding the effects of land cover pattern on land surface temperature in urban landscapes. Landsc Urban Plan 102: 54–63
Zhou W, Qian Y, Li X, Li W, Han L (2014) Relationships between land cover and the surface urban heat island: seasonal variability and effects of spatial and thematic resolution of land cover data on predicting land surface temperatures. Landsc Ecol 29:153–167